Journal of Molecular Medicine (2024) 102:1457–1470
https://doi.org/10.1007/s00109-024-02491-z

JMolMed

ORIGINAL ARTICLE

Umbelliferone alleviates impaired wound healing and skin barrier dysfunction in high glucose-exposed dermal fibroblasts and diabetic skins

Dong Yeon Kim[1] · Young-Hee Kang[2] · Min-Kyung Kang[1]

Received: 13 March 2024 / Revised: 9 August 2024 / Accepted: 18 September 2024 / Published online: 4 October 2024
© The Author(s) 2024

Abstract

Skin wound healing is a complex process involving various cellular and molecular events. However, chronic wounds, particularly in individuals with diabetes, often experience delayed wound healing, potentially leading to diabetic skin complications. In this study, we examined the effects of umbelliferone on skin wound healing using dermal fibroblasts and skin tissues from a type 2 diabetic mouse model. Our results demonstrate that umbelliferone enhances several crucial aspects of wound healing. It increases the synthesis of key extracellular matrix components such as collagen I and fibronectin, as well as proteins involved in cell migration like EVL and Fascin-1. Additionally, umbelliferone boosts the secretion of angiogenesis factors VEGF and HIF-1α, enhances the expression of cell adhesion proteins including E-cadherin, ZO-1, and Occludin, and elevates levels of skin hydration-related proteins like HAS2 and AQP3. Notably, umbelliferone reduces the expression of HYAL, thereby potentially decreasing tissue permeability. As a result, it promotes extracellular matrix deposition, activates cell migration and proliferation, and stimulates pro-angiogenic factors while maintaining skin barrier functions. In summary, these findings underscore the therapeutic potential of umbelliferone in diabetic wound care, suggesting its promise as a treatment for diabetic skin complications.

Key messages

- Umbelliferone suppressed the breakdown of extracellular matrix components in the skin dermis while promoting their synthesis.
- Umbelliferone augmented the migratory and proliferative capacities of fibroblasts.
- Umbelliferone activated the release of angiogenic factors in diabetic wounds, leading to accelerated wound healing.
- Umbelliferone bolstered intercellular adhesion and reinforced the skin barrier by preventing moisture loss and preserving skin hydration.

Keywords Dermal fibroblasts · Wound healing · Diabetic skin · Skin barrier · Skin hydration · Umbelliferone

Introduction

Impaired wound healing poses a significant health challenge, particularly among diabetic patients, with substantial implications for both health outcomes and socioeconomic burdens [1, 2]. The consequences of inadequate wound healing in diabetes are far-reaching, often culminating in infection, persistent inflammation, sepsis, wound reopening, and potentially fatal outcomes [3]. Despite the profound impact of this persistent issue, effective therapeutic interventions remain elusive. Current strategies, such as adjustments in wound dressing and the administration of growth factors and cytokines, still fall short in addressing the complex needs of diabetic wound management [2, 4, 5].

✉ Min-Kyung Kang
mkkang@anu.ac.kr

Dong Yeon Kim
ehddus7136@gmail.com

Young-Hee Kang
yhkang@hallym.ac.kr

[1] Department of Food Science and Nutrition, Andong National University, 1375, Gyeongdong-ro, Andong-si, Gyeongsangbuk-do 36729, Republic of Korea

[2] Department of Food and Nutrition, Hallym University, 1, Hallymdaehak-gil, Chuncheon-si, Gangwon-do, Republic of Korea

Diabetic wounds are characterized by an excessive influx and activation of neutrophils, impaired formation of new blood vessels (angiogenesis), and deficiencies in the movement and growth of epithelial cells [6, 7]. These deficiencies prolong the inflammatory stage of wound healing, leading to further tissue deterioration due to heightened levels of inflammatory cytokines, reactive oxygen species, and harmful enzymes [8, 9]. Angiogenesis, crucial for delivering nutrients to damaged tissue, and reepithelialization, involving the proliferation and migration of epidermal keratinocytes and dermal fibroblasts, are pivotal molecular processes in wound repair [10–12]. Hence, interventions targeting inflammation, angiogenesis, and reepithelialization hold promise for initiating the tissue-rebuilding phase of wound healing. Investigating multifaceted factors capable of concurrently influencing these processes is urgently warranted.

Umbelliferone, also referred to as 7-hydroxycoumarin, is a naturally occurring coumarin compound widely distributed in various plant species. It can be found in herbs such as sanicle, celery, cumin, fennel, parsley, hogweed, and carrots [13]. Extensive research has explored the pharmacological properties of umbelliferone, including its involvement in inflammation and oxidative stress processes [14]. Notably, this compound has shown potential in preventing hepatocyte cell death by mitigating endoplasmic reticulum stress [15]. Moreover, umbelliferone exhibits promise in slowing down the advancement of diabetic nephropathy by inhibiting ferroptosis in HK-2 cells and diabetic kidneys [16]. However, its potential in ameliorating skin wound formation associated with diabetic dermopathy remains uncertain.

In this research, we explore the impact of umbelliferone on the natural healing process of skin wounds. We elucidate the diverse functions of umbelliferone in diabetic wound healing, highlighting its ability to uphold the integrity of the extracellular matrix (ECM) and facilitate the proliferation, migration, angiogenesis, and reepithelialization of cells. Additionally, umbelliferone preserves the skin's barrier functions through improved moisturizing capabilities in both dermal fibroblasts and diabetic skin tissues. These discoveries offer promising prospects for the development of innovative, mechanism-driven therapies to address the impaired wound healing associated with diabetes.

Materials and methods

Chemicals

Human dermal fibroblast was sourced from Clonetics (San Diego, CA). Fetal bovine serum (FBS), trypsin–EDTA, and penicillin–streptomycin were provided from Lonza (Walkersville, MD, USA). Dulbecco's modified Eagle's medium (DMEM), mannitol, D-glucose, umbelliferon, and all other regents not mentioned elsewhere were obtained from Sigma-Aldrich Chemical (St. Louis, MO, USA). Horseradish peroxidase (HRP)-conjugated goat anti-rabbit immunoglobulin (Ig)G, goat anti-mouse, and donkey anti-goat IgG were acquired from Jackson ImmunoResearch Laboratories (West Grove, PA, USA). Essentially, fatty acid-free bovine serum albumin (BSA) and skim milk were supplied by Becton Dickinson Company (Sparks, MD, USA). Mouse monoclonal antibodies of collagen I (clone 3G3, catalog no. sc-293182), fibronectin (clone 2775–8, catalog no. sc-69681), pro-collagen I (clone M-60, catalog no. sc-30136), matrix metalloproteinase (MMP)-2 (clone 2C1, catalog no. sc-13594), MMP-9 (clone E-11, catalog no. sc-393859), EVL (clone B-1, catalog no.sc-376943), Fascin-1 (clone 55 K-2, catalog no. sc-21743), VEGF (clone VG-1, catalog no. sc-53462), E-cadherin (clone 5F133, catalog no. sc-71007), Occludin (clone E-5, catalog no. sc-133256), Has-2 (clone C-5, catalog no. sc-365263), HYAL (clone 1D10, catalog no. sc-101340), and AQP-3 (clone F-1, catalog no. sc-518001) were supplied by Santa Cruz Biotechnology (Santa Cruz, CA, USA). Rabbit polyclonal antibody of ZO-1 (catalog no. #61–7300) was obtained from Thermo Fisher Scientific (Waltham, MA, USA). Antibody of mouse polyclonal HIF-1α (clone D2U3T, catalog no. 3716S) was purchased from Cell Signaling Technology (Denver, MA, USA). Mouse monoclonal β-actin (clone AC-15, catalog no. A1978) antibody was provided by Sigma-Aldrich Chemical. All primary antibodies were diluted at a 1:1000 ratio in 5% BSA.

Cell culture

Human dermal fibroblasts were cultured in Dulbecco's modified Eagle's medium (DMEM) containing 10% FBS, 100 U/ml penicillin, 100 µg/ml streptomycin, and 2 mM glutamine at 37 °C in a humidified incubator containing 5% CO_2. Cells were seeding at 90% confluence in all experiments. Fibroblasts were incubated in 5.5 mM normal glucose or 33 mM high glucose for a hyperglycemia environment. Non-toxic concentrations of 1–20 µM umbelliferone were added in media for 3 days. Cell viability or cytotoxicity was measured by assaying with MTT assay (3-(4,5-dimethylthiazol-2-yl)-2,5-diphenyltertrazolium bromide). Cells were incubated with 1 mg/ml MTT solution at 37 °C for 3 h, forming an insoluble purple formazan product that was dissolved in isopropanol prior to reading the absorbance in a microplate reader at 570 nm.

In vivo animal experiments

Male C57BL/6 J mice of 5 weeks of age (average weight 20 ± 0.5 g) were purchased from DooYeol Biotech (Seoul,

Korea). To introduce diabetes, mice were subjected to daily intraperitoneal (IP) injections of streptozotocin (STZ) (Sigma-Aldrich Chemical, St. Louis, MO, USA) dissolved in sodium citrate buffer (pH 4.5, 25 mg/kg/day) for five consecutive days. The induction of diabetes was confirmed by a fasting blood glucose concentration after the fifth day of STZ injection, and mice were divided into three subgroups ($n = 9$–10 for each subgroup). The first group was fed a standard laboratory chow diet (DooYeol Biotech, Seoul, Korea) as a control. The STZ-treated mice fed a high-fat diet (HFD) were divided randomly into two groups based on fasting glucose checks. One group received water orally after STZ administration, while the other group received oral administration of umbelliferone at a dosage of 10 mg/kg body weight for 10 weeks, excluding the day of wound formation and the following 2 days. The content in fat percentage of the diets is 60% kcal% fat. Mice were kept on a 12-h light/dark cycle at 23 ± 1 °C with 50 ± 10% relative humidity under specific pathogen-free conditions, fed a standard laboratory chow diet (CJ Feed, Seoul, Korea), and were provided with water ad libitum at the animal facility of Hallym University. All experiments were approved by the Committee on Animal Experimentation of Hallym University and performed in compliance with the University's Guidelines for the Care and Use of Laboratory Animals (hallym(2023–18)). No mice died, and no apparent signs of exhaustion were observed during the experimental period.

Full-thickness excisional wound model

Mice were anesthetized with 250 mg/kg concentration of Avertin via intraperitoneal injection. After anesthesia, the dorsal hair was shaved to fully expose the skin, which was then rinsed with 70% ethanol. Four full-thickness wounds were created on each mouse using a 6-mm-diameter biopsy punch under sterile conditions. To determine the wound closure rate, wound areas were evaluated on days 0, 4, 8, 12, 14, and 18 post-wounding. Photographs were taken, and the wound area was measured by tracking the edge of the wound using ImageJ image analysis software (NIH, Bethesda, MD, USA). The percentage of wound closure was expressed as the ratio of the remaining area of the wound to the original area of the wound over time. The percentage of residual scar rate was expressed by taking the ratio of the scar area to the original area of the wound.

Western blot analysis

Whole-cell lysates were prepared from fibroblasts (3.5×10^5 cells) and skin tissue extracts from mouse skin using RIPA buffer. The skin tissue extracts were obtained from the skin of mice that were grown until 10 weeks. After anesthesia, skin samples from mice were collected from the mice, immediately extracted, and snap-frozen for biochemical assays. For western blot analysis, each sample was homogenized in lysis buffer and centrifuged at 3000 rpm for 10 min to remove any insoluble material. The supernatant was then transferred to a clean tube. Protein concentration was determined using the Lowry protein assay, and 30–50 μg of protein was used for the experiments. Equal amounts of proteins from cell lysates and tissue extracts were separated by electrophoresis on 8–12% SDS-PAGE and then transferred onto a nitrocellulose membrane. Nonspecific binding was blocked with either 3% fatty acid-free bovine serum albumin (BSA) or 5% nonfat dry skim milk for 3 h. The membrane was subsequently incubated overnight at 4 °C with primary antibodies targeting specific proteins, followed by washing in a TBS-T buffer for 10 min. Afterward, the membrane was incubated for 1 h with secondary antibodies (goat anti-rabbit IgG, goat anti-mouse IgG, or donkey anti-goat IgG) conjugated to HRP. Each target protein level was assessed using immobilon western chemiluminescent horseradish peroxidase substrate (Millipore Corp.) and detected through chemiluminescence using a ChemiDoc (Cytiva). Additionally, incubation with a mouse monoclonal β-actin antibody was performed for comparative controls. We performed a quantitative analysis of the western blot results using densitometry. The band intensities were measured using ImageJ software (NIH, Bethesda, MD, USA) and normalized to the corresponding β-actin bands. The relative expression levels were calculated and statistically analyzed.

Immunostaining

Fibroblasts were fixed with 4% formaldehyde for 10 min and permeabilized by 0.1% Triton X-100 on ice. To blockade the unspecific protein binding, fibroblasts were treated with 5% bovine serum albumin (BSA) for 1 h. The primary antibody for collagen I was prepared by diluting it at a ratio of 1:100 in 5% BSA and incubated overnight at 4 °C. The secondary antibody, Cy3-conjugated anti-mouse IgG (Sigma-Aldrich Chemical, St. Louis, MO, USA), was diluted at a ratio of 1:500 in PBS and used for the cytochemical staining of fibroblasts for 30 min. Nuclear staining was performed using 4′,6-diamidino-2-phenylindole (DAPI), which was diluted at a ratio of 1:1000 in PBS. Slide was mounted in glycerol (Sigma-Aldrich Chemical, St. Louis, MO, USA). Images were taken using an inverted microscope system for the visualization of collagen I (Nikon, Tokyo, Japan). Fluorescence intensity of immunostained cells, using a Cy3-red dye, was measured with the ImageJ software (National Institutes of Health, Bethesda, MD, USA). The red channel of the images was analyzed directly. Regions of interest (ROIs) corresponding to individual cells were selected. The mean fluorescence intensity within each ROI was quantified, and background fluorescence was subtracted. The results were

normalized to control samples to account for variability between experiments.

Cell scratch wound healing assay

To evaluate the impact of glucose on dermal fibroblast motility, as well as the potential effects of umbelliferone, an in vitro scratch wound assay was employed. In this assay, fibroblasts were seeded onto a 12-well plate and allowed to incubate for 24 h in media containing 10% FBS (fetal bovine serum). Once the cells reached confluency, a scratch was created horizontally in each well using a pipette tip. After the scratch was made, the injured cells were further incubated for an additional 24 h in culture media containing 33 mM high glucose media, with or without the presence of 1–20 μM umbelliferone. Images of scratch wounds were captured in 2–3 microscopic fields per well using a microscope equipped with a Nikon camera (Nikon, Tokyo, Japan). Quantification of wound closure was performed using ImageJ software (NIH, Bethesda, MD, USA) normalized with the wound size at day 0 as 100%.

Rhodamine phalloidin staining

Fibroblasts (0.7×10^5 cells) were fixed with 4% formaldehyde for 10 min and permeabilized with 0.1% Triton X-100 for 10 min on ice. For red cytochemical staining, the cells were treated with red-fluorescent rhodamine phalloidin (Thermo Fisher Scientific, Waltham, USA) for 30 min. Nuclear counterstaining was performed using 4′,6-diamidino-2-phenylindole (DAPI). Each slide was mounted with VectaMount mounting medium (Vector Laboratories, Burlingame, CA, USA).

Hematoxylin and eosin staining of skin tissue and measurement of epidermis/dermis thickness and adipocyte size

Paraffin-embedded skin specimens were cut into 8 μM thick sections, dewaxed and rehydrated, and stained with eosin reagent to assess and hematoxylin for counterstaining. The stained tissue slides were examined using a microscope equipped. The thickness of skin epidermis, dermis, and adipocyte size were analyzed by ImageJ software.

Masson and Gomori trichrome staining

For the histological analysis, the skin was obtained at the end of the experiments and fixed in 10% buffered formalin. The skin tissues were then embedded in paraffin, and sections of 8 μM thickness were prepared. These sections were de-paraffinized and stained with Masson and Gomori trichrome to visualize collagen fibers and muscle fibers under light microscopy. The stained tissue sections were examined using an inverted microscope system. The analysis of Masson and Gomori staining intensity was performed using ImageJ software. Digital images were uploaded to ImageJ, and a scale was set using digital micrometer gauge readings to convert pixel units to microns. The proportions of collagen fibers (blue areas), cytoplasm, and muscle (red areas) were determined by setting the appropriate color thresholds, following the methodology [17].

In vivo skin evaluation

Hydration and TEWL of the dorsal skin of the mice were measured with a Corneometer CM 825 (Courage and Khazaka, Köln, Germany), and SCH was measured using GPSkin (GPOWER Inc., Seoul, South Korea), respectively. Three independent measurements from the same area of skin were averaged for each value.

Statistical analysis

Data were analyzed using SPSS (SPSS Inc., Chicago, IL, USA), and a mean difference of $p < 0.05$ was considered statistically significant. Different letters in the figures indicate significant differences between various treatment groups at $p < 0.05$, as determined by one-way ANOVA. Once a significant difference was recognized, Tukey's test was conducted as a post hoc analysis to compare the differences between the groups. All data are presented as mean ± SD.

Results

Umbelliferone induces dermal fibroblast collagen synthesis, paralleled decreased activation of MMPs under high glucose setting

To study the impact of high glucose environment on skin dermal fibroblasts ECM compositions, dermal fibroblasts were exposed to 33 mM glucose for 6 days. A temporal downregulated expression of cellular ECM components, collagen I and fibronectin, was observed in dermal fibroblasts (Fig. 1E). Furthermore, results from rhodamine phalloidin staining were employed to observe changes in the cellular morphology of fibroblasts. It was observed that fibroblasts exposed to high glucose exhibited more simplified morphology, showing an approximate 30.95 ± 10.3% reduction in length compared to their original state (Fig. 1D). Exposure of fibroblasts to hyperglycemia adding with 1–20 μM umbelliferone for 3 days, the induction of pro-collagen I, collagen I, and fibronectin was inclined (Figs. 1F, 2A) and there was no cytotoxicity observed from the MTT assay (Fig. 1B, C).

The matrix metalloproteinase (MMP) proteins cause the degradation of ECM components via aberrant proteolysis of cells, leading to cellular dysfunctions. The expression of MMP-2 and MMP-9 was elevated following the high glucose stimulation, which was attenuated by umbelliferone (Fig. 2B).

Under normal glucose conditions, fibroblasts exhibited robust cytoplasmic red staining, as confirmed by collagen I immunocytochemical staining (Fig. 2C). However, exposure to hyperglycemic conditions for 3 days led to a reduction in cellular levels of collagen I. Conversely, treatment with umbelliferone at concentrations of ≥ 10 μM augmented the suppression of collagen I induction caused by high glucose insult.

Histopathological alterations of skin tissue in diabetic mellitus

This study also confirmed changes in extracellular matrix (ECM) component proteins induced by streptozotocin in a type 2 diabetic mouse model using western blot analysis. Both collagen type I and fibronectin exhibited a decrease in the diabetic group, as observed in cell experiments. However, upon administration of umbelliferone, an increase in ECM components was observed (Fig. 2D). Furthermore, additional analysis involved Masson and Gomori trichrome staining, selectively staining collagen fibers blue in the tissue (Fig. 3C, D). The results revealed a substantial reduction in intensely stained blue collagen fibers in diabetic mice compared to the control group. Conversely, upon umbelliferone treatment, collagen fiber synthesis became more active, represented by lighter blue staining, and the optical density of blue collagen fibers was depicted using a bar graph (Fig. 3H, I). In contrast, when examining matrix metalloproteinases (MMPs) through western blot analysis, enzymes responsible for ECM component degradation, it was observed that the activity of MMP2 and MMP9, which were pronounced in diabetic mice, decreased upon umbelliferone treatment (Fig. 2E).

Hematoxylin and eosin (H&E) staining was performed on skin tissues from diabetic-induced mice. An overall image of the skin tissue, ranging from the epidermal layer to the muscular layer, is presented (Fig. 3A). Additionally, micrographs displaying magnified views of the epidermis and dermal layers are shown (Fig. 3F, G). In the skin tissue of mice induced by streptozotocin, compared to the control group, an increase in adipocyte size was observed (Fig. 3A, E), along with an augmented epidermal thickness (Fig. 3B, F), and a decrease in overall dermal thickness (Fig. 3B, G). Conversely, in the group treated with umbelliferone, a relatively reduced adipocyte size was evident, and both epidermal and dermal thickness were restored to levels similar to the control group.

Enhancement of cell motility by umbelliferone

We investigated alterations in proteins associated with cellular migration of fibroblasts under chronic hyperglycemia condition. Fibroblasts cultivated in a high glucose environment of 33 mM demonstrated a marked decrease in the expression of both EVL and Fascin-1 proteins when compared to the control group. However, subsequent treatment with umbelliferone at varying concentrations exhibited a concentration-dependent augmentation in protein expressions. To evaluate both cellular motility and wound healing proficiency, a scratch wound healing assay was conducted on the fibroblasts. Microscopic images were captured after generating uniform-sized and length of scratch wounds using a yellow tip (Fig. 4B). Post-wound induction and subsequent exposure to 33 mM glucose and different concentrations of umbelliferone, it was noted that the control group exhibited heightened cell migration compared to the immediate post-scratch image (indicated by the black dotted line). Conversely, cells exposed to elevated glucose levels displayed markedly reduced migration. Notably, treatment with umbelliferone led to a concentration-dependent enhancement in cell migration, correlating with an improvement in wound healing capacity (Fig. 4C). The extent of the cellular wound area was quantified as a percentage and illustrated graphically for each experimental group (Fig. 4D).

Furthermore, we employed western blot analysis using animal skin tissues to ascertain the protein expression associated with cellular migration, which was also confirmed through in vitro experiments. Both EVL and Facsin-1 proteins exhibited reduced expression in skin tissues of streptozotocin-induced type 2 diabetic mice. However, in the groups that received oral administration of 10 mg/kg umbelliferone, protein expression increased (Fig. 4E).

Improvement of diabetic cutaneous wound healing ability by umbelliferone

The diagram illustrates the overall flow of the animal experiment (Fig. 5A). To assess the extent of wound healing ability in diabetes-induced animals, a partial removal of fur was performed on the mouse dorsum, and wounds were created using a 6 mm punch. The healing process was then observed through photographs from the day of injury until the 18th day (Fig. 5B). The wound-healing effect of umbelliferone was investigated in full-thickness cutaneous wounds in diabetic mouse. As shown in Fig. 5B, skin wounds in diabetic mice treated with umbelliferone healed more rapidly than those in untreated diabetic mice. By day 8, umbelliferone-treated mice wounds achieved nearly 25% closure compared with the 60% wound closure observed in control. On day 12, as quantified in the graph, it was confirmed that wound healing ability in mice treated with umbelliferone was approximately

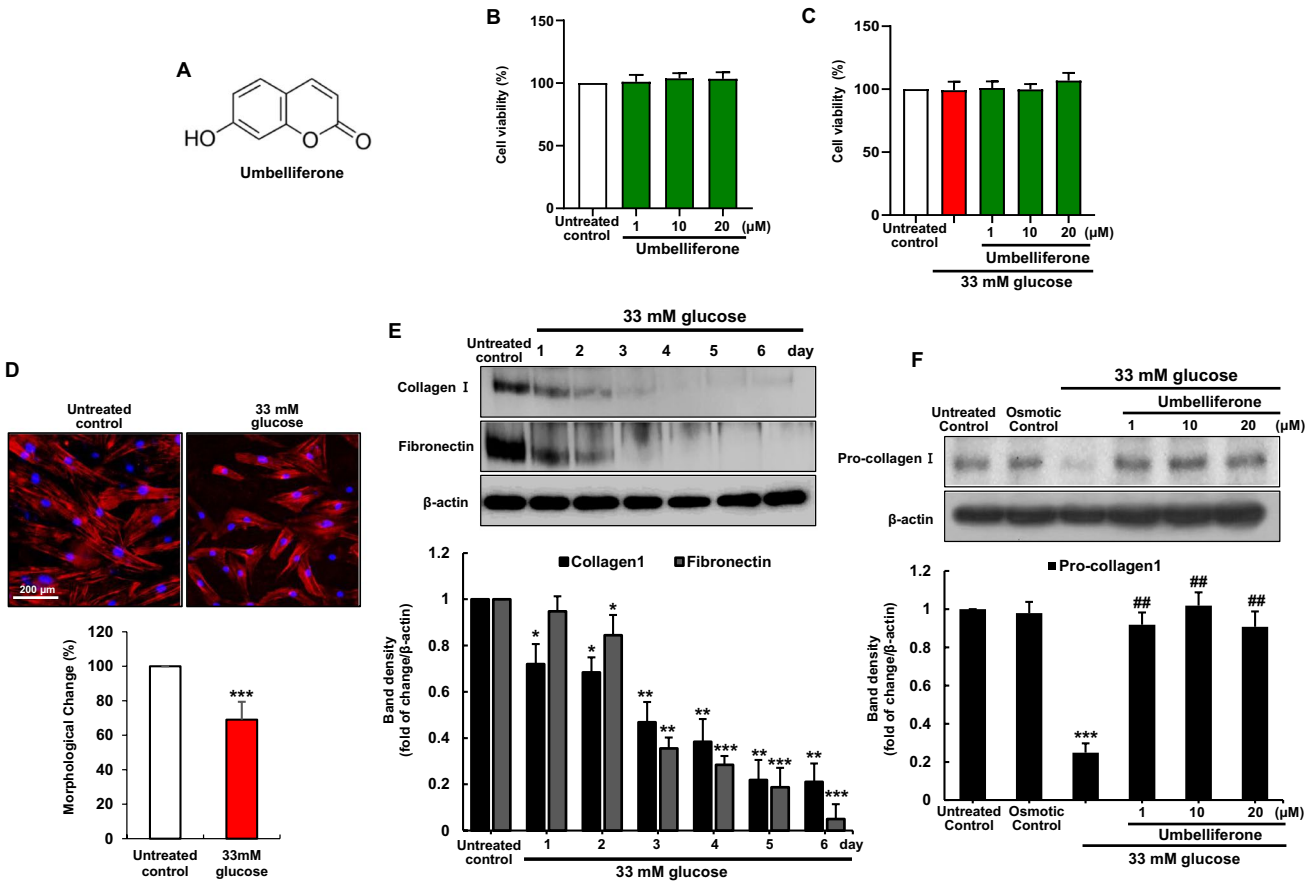

Fig. 1 Chemical structure of umbelliferone (**A**), umbelliferone cytotoxicity (**B**), and umbelliferone viability in high glucose-exposed human skin dermal fibroblasts (**C**). Cell viability was measured by the water-soluble tetrazolium salt cell quantification method (**B**, **C**). Microscopic images depicting changes in the cellular morphology of fibroblasts through rhodamine phalloidin staining (**D**). Temporal course of collagen I and fibronectin in high glucose stimulation (**E**) and induction of pro-collagen I were measured by western blot (**F**). Fibroblasts were incubated in media containing 5.5 mM glucose, 5.5 mM glucose plus 27.5 mM mannitol as osmotic controls, or 33 mM glucose in the absence and presence of 1–20 μM umbelliferone for 3 days. The bar graphs represent the quantitative results of blot bands (**E**, **F**). Densitometric analysis of immunoblots for each protein relative to β-actin is presented. Significance levels are indicated as follows: $*p<0.05$, $**p<0.01$, $***p<0.001$ for comparisons between the 33 mM glucose and control groups; $\#\#p<0.01$ for comparisons between the 33 mM glucose and umbelliferone-treated groups. Statistical significance of the mean values for each group was determined using ANOVA followed by Tukey's test. Data are expressed as means ± SD

twice as fast as in diabetic mice (Fig. 5C). On day 14, the wound healing ratio of umbelliferone-treated mice was 80%, showing a higher healing rate compared to diabetic mice.

Angiogenesis is essential for the wound healing process, involving the creation of new blood vessels from existing ones [18]. It occurs as these vessels invade the wound clot and organize into a microvascular network within the granulation tissue. Therefore, the expression of factors involved in angiogenesis, namely HIF-1α and VEGF proteins, was examined. It was observed that the secretion of these factors decreased in fibroblasts treated with high glucose and the expression of these proteins in the skin tissues of diabetic mice. Conversely, upon umbelliferone treatment, the protein secretion and expression were restored, respectively (Fig. 5D, E).

Blockade of impairment of skin junction barrier integrity and moisture retention capacity by umbelliferone

Alongside the wound healing process, we verified the expression of E-cadherin, ZO-1, and Occludin with western blot analysis, which plays a pivotal role in forming defense skin barriers within cells and tissues through adherent junctions (AJ) and tight junctions (TJ). Under hyperglycemic conditions, a reduction in protein expression of these junctional markers was observed, indicating a weakening of intercellular adhesion function [19]. Conversely, treatment with umbelliferone led to an increased expression of these proteins, confirming the reinforcement of intercellular adhesion function (Fig. 6A). The expression of cell

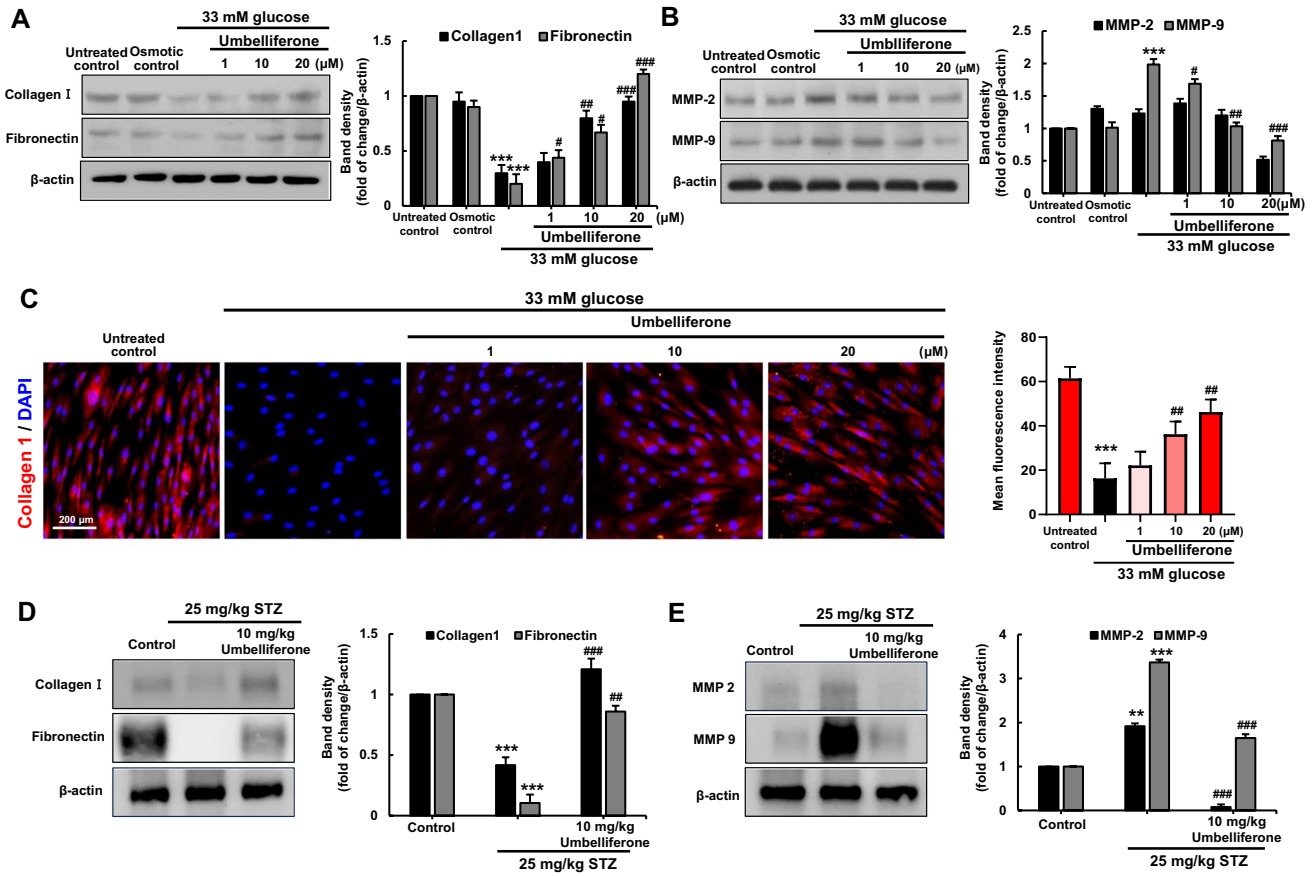

Fig. 2 Umbelliferone improved the level of multiple ECM components and deterred MMP activity in skin dermal fibroblasts and diabetic skin tissues. Western blot data showing elevation of induction of collagen I and fibronectin (**A**) and downregulated induction of MMP2 and MMP9 (**B**). Fibroblasts were incubated in media containing 5.5 mM glucose, 5.5 mM glucose plus 27.5 mM mannitol as osmotic controls, and 33 mM glucose in the absence and presence of 1–20 μM umbelliferone for 72 h. For the immunocytochemical analysis of collagen I, a red Cy3-conjugated secondary antibody was used for visualizing collagen I induction, being counterstained with 4′,6-diamidino-2-phenylindole for the nuclear staining (**C**). Each microphotograph was obtained by using a microscope system (scale bar: 200 μM). Skin tissue levels of collagen I, fibronectin (**D**), and MMP-2/9 (**E**) were measured by western blot analysis, respectively. The right bar graphs represent the quantitative results of blots in **A**, **B**, **D**, and **E**. $^{**}p<0.01$, $^{***}p<0.001$ for comparisons between the 33 mM glucose and control groups; $\#p<0.05$, $\#\#p<0.01$, $\#\#\#p<0.001$ for comparisons between the 33 mM glucose and umbelliferone-treated groups. Statistical significance of the mean values for each group was determined using ANOVA followed by Tukey's test. Data are expressed as means ± SD

adhesion-related proteins in the skin tissues of diabetic mice was confirmed, and the results were consistent with those observed in the cell experiments (Fig. 6B).

To investigate changes in the protein expression related to the moisture-retention capability of dermal fibroblasts under chronic hyperglycemia conditions, the expression of HAS2, HYAL, and AQP3 proteins was examined using western blot analysis (Fig. 6C). HAS2 is an enzyme involved in hyaluronic acid synthesis, contributing to the formation of the skin's moisture barrier and the maintenance of elasticity. On the other hand, the enzyme HYAL is a protein responsible for hyaluronic acid degradation, in contrast to HAS. AQP3 is a water transporter protein that facilitates the passage of water from fibroblasts into skin tissues. Under hyperglycemia conditions, it was observed that the HYAL showed increased activity, the expression of the induction of HAS2 protein decreased, and the ability of AQP3 protein was also diminished. However, in fibroblasts treated with umbelliferone, it was observed that the expression of the AQP3 protein increased, and the protein expression of HAS2 also increased in a concentration-dependent manner. Conversely, the expression of the HYAL protein declined. In mice induced with diabetes by streptozotocin, the western blot analysis of protein expression related to skin moisture retention yielded results consistent with cell experiments (Fig. 6D). In STZ-induced mice, the HYAL protein showed a significant increase compared to the control, while the HAS2 and AQP3 proteins were observed to decrease. However, oral administration of umbelliferone resulted in the recovery of these proteins to the control group levels. We also measured the degree of skin water loss through the mice skin tissues,

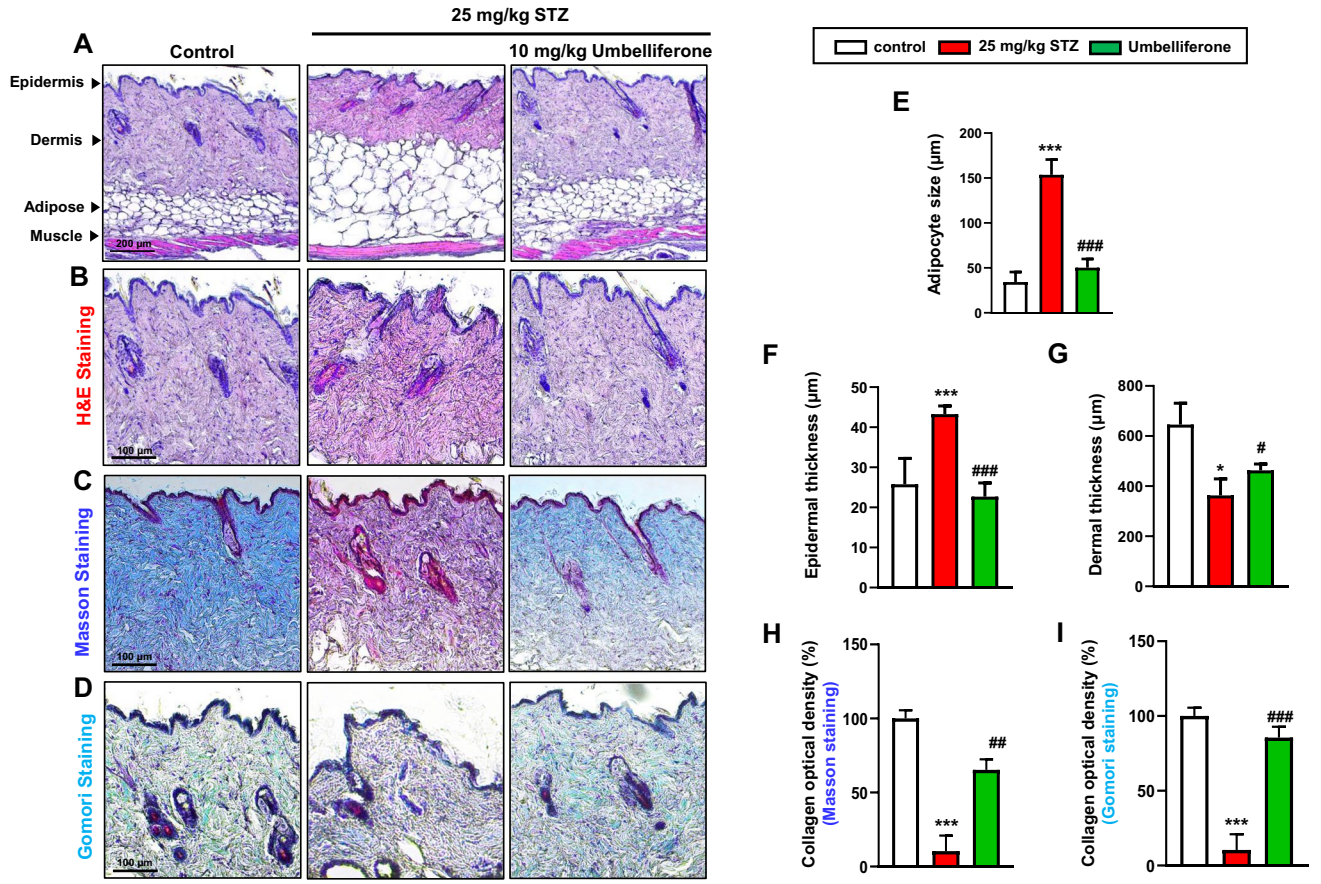

Fig. 3 Representative images of hematoxylin and eosin (H&E) and Masson's and Gomori trichrome-stained histological sections from skin dorsal of mice from different treatment groups. Images of the epidermis, dermis, subcutaneous adipose tissue, and muscular layer of skin tissue (**A**). Below are focused images of the epidermis and dermal regions (**B**). The reddish staining indicates cytoplasm and muscle fibers, and the blue staining shows collagen fibers and connective tissues (**C**, **D**). Bar graph of subcutaneous adipocyte size (**E**), epidermal thickness (**F**), dermis thickness (**G**), and collagen fiber optical density (**H**, **I**). $*p<0.05$, $***p<0.001$ for comparisons between STZ-induced diabetic mice and control groups; $\#p<0.05$, $\#\#p<0.01$, $\#\#\#p<0.001$ for comparisons between STZ-induced diabetic mice and STZ-induced diabetic mice treated with umbelliferone. Statistical significance of the mean values for each group was determined using ANOVA followed by Tukey's test. Data are expressed as means ± SD

represented by epidermal water loss (Fig. 6E), the moisture content in the outermost layer of the skin, referred to as skin stratum corneum hydration (SCH) (Fig. 6F), and the skin's humidity (Fig. 6G). In diabetic mice, we observed a significant increase in skin water loss through the epidermis compared to the control group, while the moisture content in the stratum corneum and skin humidity were significantly decreased. However, the administration of umbelliferone resulted in an increase in skin moisture retention capability and a suppression of moisture evaporation.

Discussion

Complications arising from impaired wound healing can result in foot ulcers and, in severe cases, may necessitate amputation, making diabetic mellitus a significant contributor to mortality rates [3, 6]. The wound healing process unfolds through four distinct stages: hemostasis, inflammation, proliferation/migration, and remodeling. Hyperglycemia can impede wound healing, thereby prolonging this cascade of events. Dermal fibroblasts, key cellular components of the skin's dermis, play a vital role in wound healing by aiding in the synthesis of extracellular matrix (ECM) components, facilitating the production of factors essential for neovascularization, and orchestrating the remodeling of the wound site through cellular growth and migration [20, 21]. Consequently, holistic therapeutic strategies targeting these aspects of wound healing may hold considerable promise for enhancing diabetic skin wound recovery. In the present study, we demonstrated that umbelliferone ameliorated diabetes-associated delayed skin wound healing and improved skin barrier functions both in vitro and in vivo.

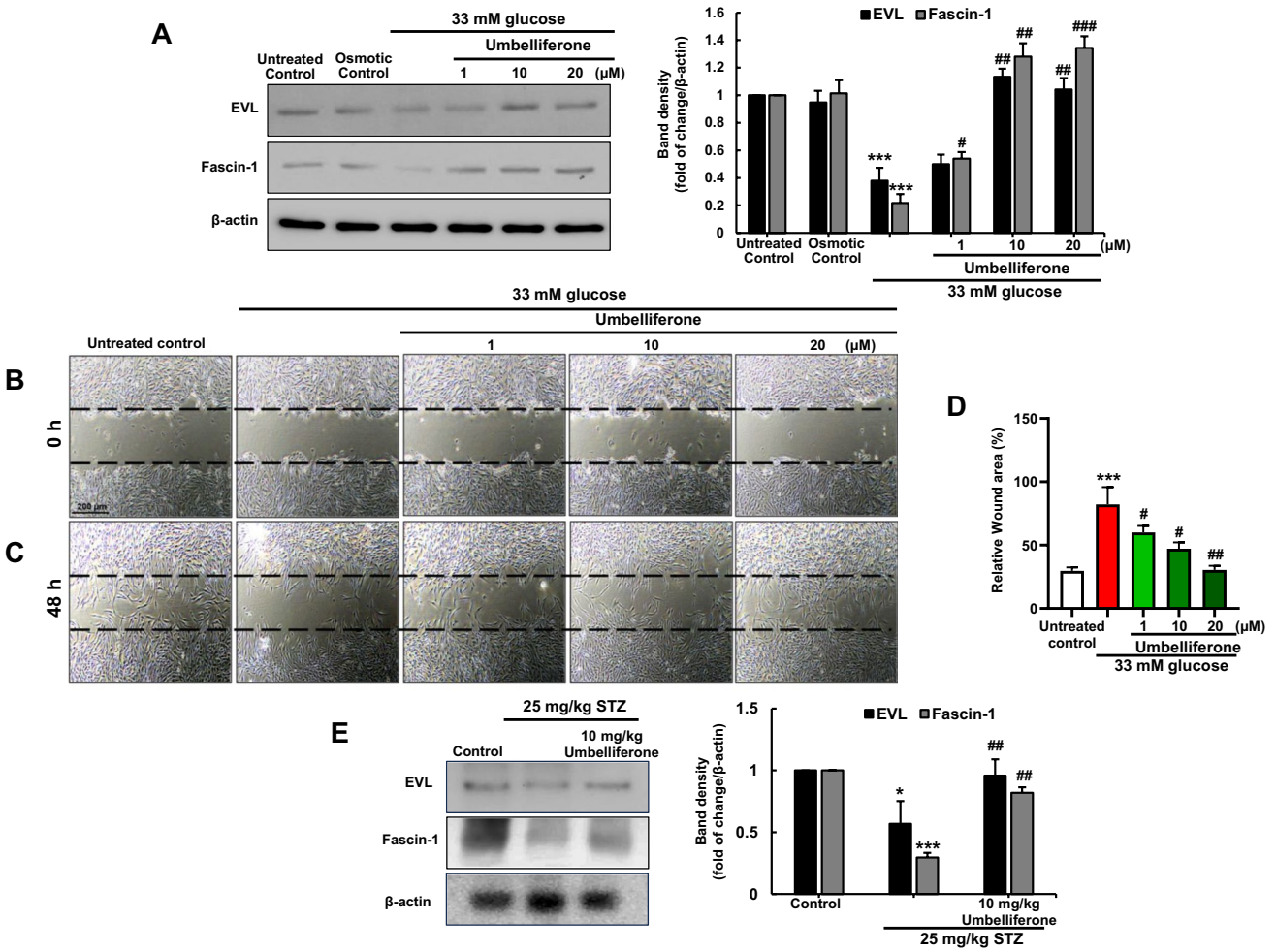

Fig. 4 Umbelliferone improves cell migration and motility markers induced by high glucose stimulation. Fibroblasts were cultured in high glucose media with or without umbelliferone for 3 days. EVL and Fascin-1 levels were assessed by western blot assay (**A**). Scratch wound healing assays were performed to examine fibroblast migration in the hyperglycemia condition with or without 1–20 μM umbelliferone (**B**, **C**). Microscopic images were captured immediately after inducing a scratch, with the initial scratch size indicated by white dots (**B**). Subsequently, images were taken 48 h after scratch induction, following treatment with high glucose and umbelliferone of varying concentrations (**C**). The graph represents the scratch area as a percentage (**D**). The skin tissue levels of EVL and Fascin-1 were measured by western blot (**E**). The right bar graphs represent the quantitative results of blots in **A** and **E**. *$p<0.05$, ***$p<0.001$ for comparisons between the 33 mM glucose/diabetic mice and control groups/control mice; #$p<0.05$, ##$p<0.01$, ###$p<0.001$ for comparisons between the 33 mM glucose/diabetic mice and umbelliferone-treated groups. Statistical significance of the mean values for each group was determined using ANOVA followed by Tukey's test. Data are expressed as means ± SD

The skin dermis serves as the architectural framework of the skin, imparting robustness and suppleness while accommodating various essential components like hair follicles, glands, blood vessels, and nerves. At the heart of dermal function are the dermal fibroblasts (DF), primary cells responsible for orchestrating the synthesis of the extracellular matrix (ECM), thereby providing structural integrity and support to the skin tissue [22]. DFs exhibit remarkable plasticity throughout skin development, wound healing, regeneration, and skin disease pathology [23]. Also, fibroblasts play a crucial role in the repair of cutaneous wounds by migrating to the site of damage, replenishing the wounded area, and restructuring fibrin and collagen deposits [24]. They induce biochemical alterations in the extracellular matrix (ECM) by breaking down fibrin and synthesizing collagen, playing a significant role in the contraction of granulation tissue [21]. The ECM molecules play an indispensable role in initiating the proliferation, migration, and interactions of diverse cells within skin tissues [25]. The interaction and balance between ECM components and MMPs are crucial for maintaining skin stability, as they play a pivotal role in the deposition, maturation, and reorganization of the extracellular matrix (ECM) during the wound healing process [26, 27]. However, increased activities of MMPs have been noted in diabetic wounds, which can directly decrease collagen, consequently disrupting the healing process. In our

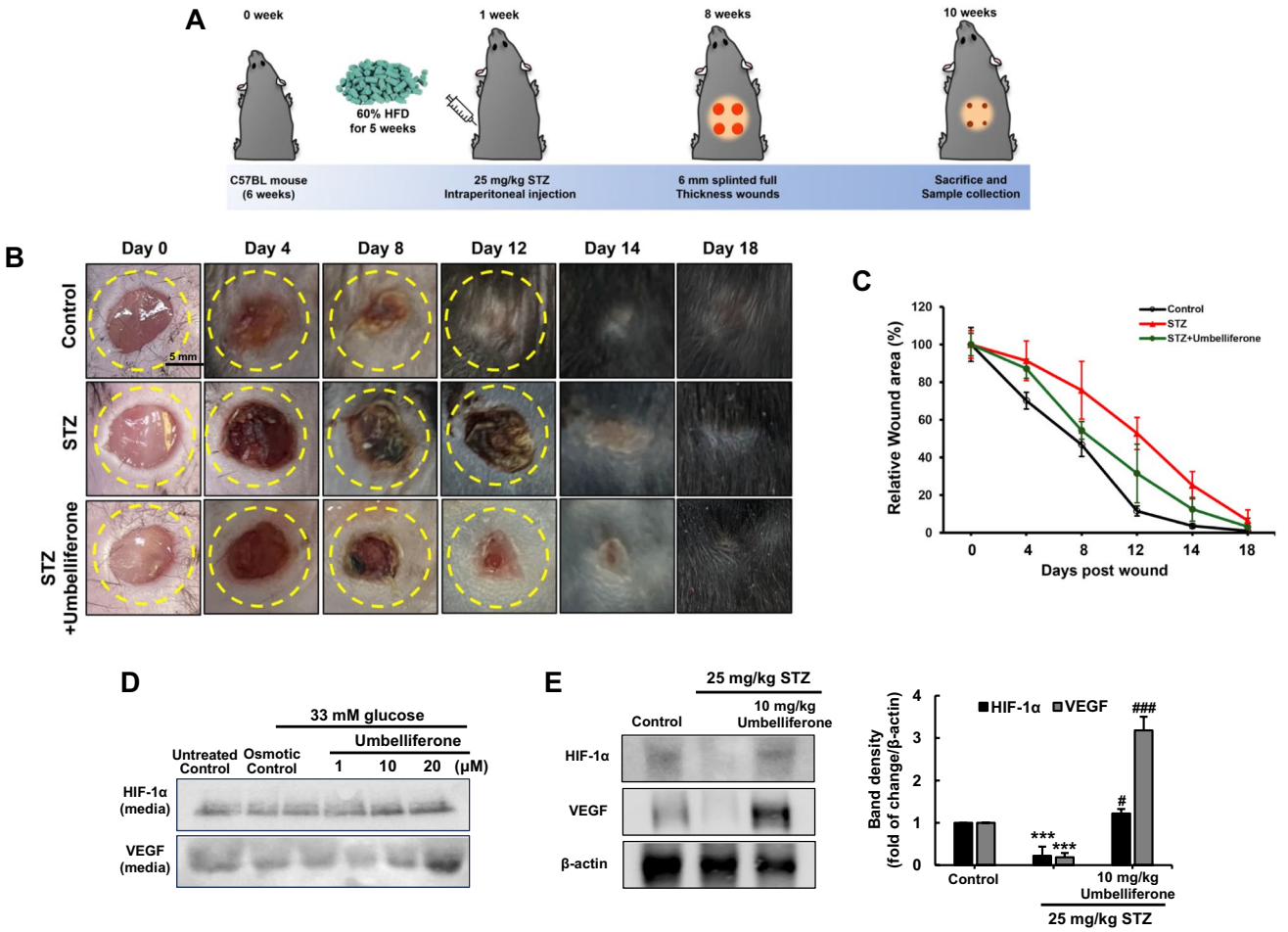

Fig. 5 Schematic diagram outlining the animal experimental procedure (**A**). Following a 1-week period of STZ injection, mice were subjected to a 6 mm circular wound on their dorsal using a punch biopsy. Images of the wound were captured at intervals of 4 days until day 18, facilitating observation of wound progression. Representative images demonstrating wound closure were captured on specific days: day 0, day 4, day 8, day 12, day 14, and day 18 (**B**), and the quantitative analysis of the percentage of wound closure was conducted (**C**). Western blot analysis was conducted on fibroblasts (**D**) and diabetic skin tissue (**E**) to examine the levels of HIF-1α and VEGF proteins. The right bar graphs represent the quantitative results of blots in **E**. ***$p < 0.001$ for comparisons between the diabetic mice and control mice; #$p < 0.05$, ###$p < 0.001$ for comparisons between the diabetic mice and umbelliferone-treated groups. Statistical significance of the mean values for each group was determined using ANOVA followed by Tukey's test. Data are expressed as means ± SD

results, we observed a decrease in ECM components and an increase in MMP activity in high glucose-induced fibroblasts and diabetic skin tissues. However, treatment with umbelliferone was found to restore the expression of collagen I and fibronectin while reducing the expression of MMP-2 and MMP-9. Additionally, we found an increase in accumulated collagen fibers with strong blue staining following the administration of umbelliferone, which had decreased in diabetic mice.

The cell proliferation, crucial for tissue repair, plays a vital role in facilitating wound closure in biological systems. Migration is equally essential for effective wound contraction and the formation of granulation tissue, which are critical for successful wound healing [28]. Fascin-1 promotes cell movement by bundling actin filaments, particularly aiding in filopodia formation [29, 30]. Ena-VASP-like (EVL), located at filopodia tips and adhesive sites, regulates cell morphology and movement, impacting developmental angiogenesis in the postnatal retina [31]. Depletion of EVL reduces endothelial tip cell density and impairs vascular sprouting by hindering filopodia formation at the angiogenic front [32]. A notable characteristic of the proliferative phase in wound healing is robust angiogenesis, driven by various proangiogenic factors produced within wounds in response to the established oxygen gradient caused by injury which disrupts homeostasis, leading to a hypoxic state [12]. Following injury, hypoxia triggers the activation of hypoxia-inducible factor-1(HIF-1α), a transcriptional activator

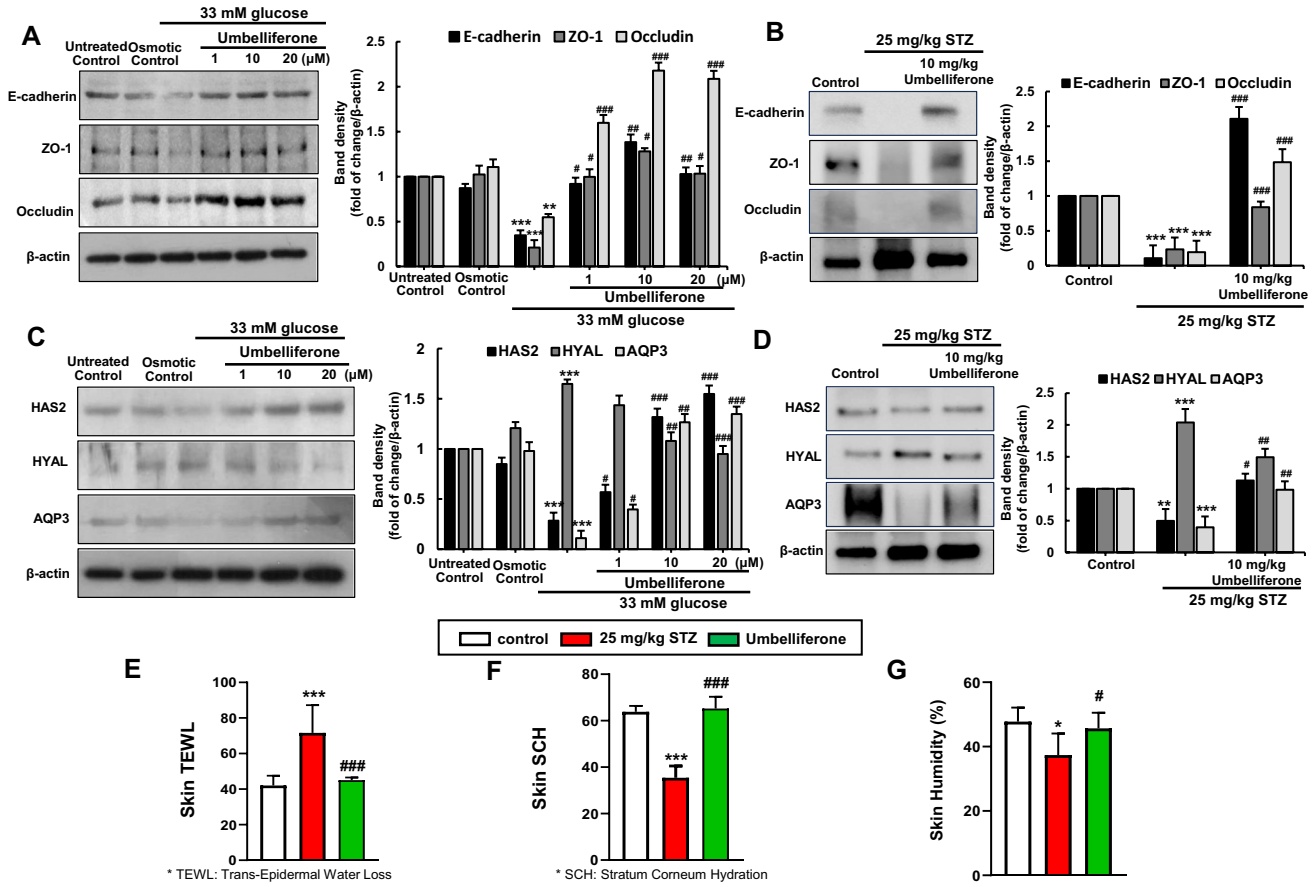

Fig. 6 Western blot analysis of E-cadherin, ZO-, and Occludin in fibroblasts (**A**) and diabetic skin tissue (**B**). Alterations in the expression of proteins associated with skin tissue's moisture retention ability, namely, HAS2, HYAL, and AQP3, were examined through western blot analysis in both fibroblast cells (**C**) and skin tissue (**D**). The right bar graphs represent the quantitative results of blots in **A**–**D**. Dermal fibroblast cells were cultured in a high-glucose medium for 3 days and treated with umbelliferone at concentrations ranging from 1 to 20 μM. The animal model involved intraperitoneal streptozotocin injections for 5 days, followed by oral administration of umbelliferone for 4 weeks. The indices measured included TEWL (trans-epidermal water loss), a metric quantifying moisture evaporation through the skin (**E**); skin SCH (stratum corneum hydration), a measure of moisture content in the skin's outermost layer (**F**); and humidity, an indicator of overall skin moisture state (**G**). Measurements were conducted on the dorsal area of the mice (**E**–**G**). $*p<0.05$, $**p<0.01$, $***p<0.001$ for comparisons between the 33 mM glucose/diabetic mice and control groups/control mice; $\#p<0.05$, $\#\#p<0.01$, $\#\#\#p<0.001$ for comparisons between the 33 mM glucose/diabetic mice and umbelliferone-treated groups. Statistical significance of the mean values for each group was determined using ANOVA followed by Tukey's test. Data are expressed as means ± SD

that stimulates angiogenesis by increasing the expression of target genes such as vascular endothelial growth factor (VEGF) [33]. The secretion of pro-angiogenic molecule VEGF by fibroblasts promotes the formation of new blood vessels, which is a crucial mechanism in tissue regeneration [34]. Throughout this interconnected process, wound contraction takes place. Our study confirmed that under diabetic conditions, impaired cell growth and migration, along with suppressed activity of angiogenic factors, contribute to delayed wound healing. This was validated not only through cell scratch assays but also through experiments involving intentionally created wounds on the dorsal area of mice. However, we observed that umbelliferone promotes cell migration and growth in response to hyperglycemic stimuli. Furthermore, we confirmed an increase in the secretion of angiogenesis-promoting factors, including HIF-1α and VEGF, suggesting the wound-healing potential of umbelliferone.

The skin barrier protects against pathogens, chemicals, and water loss, relying on components like the microbiome, tight junctions, and chemical and immunological barriers [35, 36]. The barrier breakdown leads to increased water loss and reduced skin hydration. Tight junctions are essential for barrier integrity and the remodeling phase of wound healing, and they also help maintain skin hydration [19]. The deficiency of Claudin-1 protein has been reported to result in profound water loss due to defects in the skin barrier [37]. Additionally, the knockdown of ZO-1 and Occludin proteins has been documented to increase paracellular permeability in epidermal keratinocytes for ions and large molecules [38]. Moreover, the knockdown

of Claudin-1 is known to impair the water barrier function in the stratum corneum [39]. Adequate moisturizing is vital for skin function, with hyaluronic acid (HA) in the dermis playing a key role. HA plays a crucial role in the skin's extracellular matrix, essential for hydration, nutrient exchange, and protection against free radical damage [40–42]. It also supports fundamental biological processes such as cell renewal, differentiation, and motility [43]. Furthermore, in several studies, HA has been utilized as a therapeutic tool to promote repair in damaged tissues, owing to its biocompatible hydrogel properties and its indispensability during embryonic development [44]. Therefore, maintaining a consistent level of HA is important for skin health, highlighting the significance of balancing Hyaluronan synthase-2 (HAS2), responsible for its synthesis, and Hyaluronidase (HYAL), responsible for its degradation. Also, in normal skin physiology, aquaporins (AQPs) transport both glycerol and water, thereby promoting water retention and skin hydration, which play a key role in various skin processes, and abnormalities in this channel have been observed in several skin diseases [45, 46]. Our study found that exposure to high glucose led to decreased expression of TJ proteins and skin moisturizing proteins in fibroblasts, as well as in the skin tissues of diabetic mice. Additionally, diabetic mice exhibited increased trans-epidermal water loss (TEWL) and reduced moisture content in the epidermal stratum corneum and overall skin hydration, along with changes in epidermal and dermal thickness. Treatment with umbelliferone restored epidermal and dermal thickness, maintained skin moisture, and restored the expression of cell adhesion and moisture-regulating factors. Thus, umbelliferone may enhance skin moisturizing ability and maintain the skin barrier in diabetic conditions.

Therefore, the findings of this study indicate that umbelliferone exhibits potential in addressing the delayed wound healing and skin barrier dysfunction induced by high glucose environments. Specifically, it appears to safeguard dermal hydration.

In summary, our study explored the impact of umbelliferone on wound healing in high glucose-induced dermal fibroblasts and diabetic skin tissues. We found that umbelliferone promoted ECM synthesis and collagen fiber production while inhibiting MMP activity. It also facilitated fibroblast migration and proliferation, boosted pro-angiogenesis factor expression, and enhanced skin hydration by regulating key enzymes. Additionally, umbelliferone strengthened the skin barrier by increasing moisture levels and improving cellular adhesion. Overall, these effects highlight umbelliferone's potential as a therapeutic agent for diabetic skin wound healing.

Author contribution DYK performed the majority of the experimental work in this study, analyzed data, and contributed to the writing of the manuscript; DYK and Y-HK performed experiments and analyzed the data; DYK and M-KK wrote the paper. M-KK had primary responsibility for the final content. The final manuscript was read and approved by all authors.

Funding This work was supported by the National Research Foundation of Korea (NRF) grant funded by the Korean government (2021R1I1A1A0104231611 and 2022R1I1A1A01067661).

Data availability The datasets generated and analyzed during the current study are available from the corresponding author M-KK on reasonable request.

Declarations

Ethics approval All animal procedures were reviewed and approved by the Institutional Animal Care and Use Committee of Hallym University (hallym(2023–18)).

Consent for publication The informed consent was obtained from study participants.

Conflict of interest The authors declare no competing interests.

Open Access This article is licensed under a Creative Commons Attribution-NonCommercial-NoDerivatives 4.0 International License, which permits any non-commercial use, sharing, distribution and reproduction in any medium or format, as long as you give appropriate credit to the original author(s) and the source, provide a link to the Creative Commons licence, and indicate if you modified the licensed material. You do not have permission under this licence to share adapted material derived from this article or parts of it. The images or other third party material in this article are included in the article's Creative Commons licence, unless indicated otherwise in a credit line to the material. If material is not included in the article's Creative Commons licence and your intended use is not permitted by statutory regulation or exceeds the permitted use, you will need to obtain permission directly from the copyright holder. To view a copy of this licence, visit http://creativecommons.org/licenses/by-nc-nd/4.0/.

References

1. McDermott K, Fang M, Boulton AJM, Selvin E, Hicks CW (2023) Etiology, epidemiology, and disparities in the burden of diabetic foot ulcers. Diabetes Care 46:209–221. https://doi.org/10.2337/dci22-0043
2. Nowak NC, Menichella DM, Miller R, Paller AS (2021) Cutaneous innervation in impaired diabetic wound healing. Transl Res 236:87–108. https://doi.org/10.1016/j.trsl.2021.05.003
3. Alavi A, Sibbald RG, Mayer D, Goodman L, Botros M, Armstrong DG, Woo K, Boeni T, Ayello EA, Kirsner RS (2014) Diabetic foot ulcers: part I. Pathophysiology and prevention. J Am Acad Dermatol 70(1):e1-18. https://doi.org/10.1016/j.jaad.2013.06.055. (quiz 19-20)
4. Niu Y, Li Q, Ding Y, Dong L, Wang C (2019) Engineered delivery strategies for enhanced control of growth factor activities in wound healing. Adv Drug Deliv Rev 146:190–208. https://doi.org/10.1016/j.addr.2018.06.002
5. Bai Q, Han K, Dong K, Zheng C, Zhang Y, Long Q, Lu T (2020) Potential applications of nanomaterials and technology for diabetic wound healing. Int J Nanomedicine 15:9717–9743. https://doi.org/10.2147/IJN.S276001
6. Burgess JL, Wyant WA, AbdoAbujamra B, Kirsner RS, Jozic I (2021) Diabetic wound-healing science. Medicina (Kaunas) 57:1072. https://doi.org/10.3390/medicina57101072

7. Francis-Goforth KN, Harken AH, Saba JD (2010) Normalization of diabetic wound healing. Surgery 147:446–449. https://doi.org/10.1016/j.surg.2009.04.038
8. Mosser DM, Hamidzadeh K, Goncalves R (2021) Macrophages and the maintenance of homeostasis. Cell Mol Immunol 18:579–587. https://doi.org/10.1038/s41423-020-00541-3
9. Cai Y, Chen K, Liu C, Qu X (2023) Harnessing strategies for enhancing diabetic wound healing from the perspective of spatial inflammation patterns. Bioact Mater 28:243–254. https://doi.org/10.1016/j.bioactmat.2023.04.019
10. Bi H, Li H, Zhang C, Mao Y, Nie F, Xing Y, Sha W, Wang X, Irwin DM, Tan H (2019) Stromal vascular fraction promotes migration of fibroblasts and angiogenesis through regulation of extracellular matrix in the skin wound healing process. Stem Cell Res Ther 10:302. https://doi.org/10.1186/s13287-019-1415-6
11. Okonkwo UA, DiPietro LA (2017) Diabetes and wound angiogenesis. Int J Mol Sci 18:1419. https://doi.org/10.3390/ijms18071419
12. Veith AP, Henderson K, Spencer A, Sligar AD, Baker AB (2019) Therapeutic strategies for enhancing angiogenesis in wound healing. Adv Drug Deliv Rev 146:97–125. https://doi.org/10.1016/j.addr.2018.09.010
13. Mazimba O (2017) Umbelliferone: sources, chemistry and bioactivities review. Bull Fac Pharm, Cairo Univ 55:223–232. https://doi.org/10.1016/j.bfopcu.2017.05.001
14. Germoush MO, Othman SI, Al-Qaraawi MA, Al-Harbi HM, Hussein OE, Al-Basher G, Alotaibi MF, Elgebaly HA, Sandhu MA, Allam AA et al (2018) Umbelliferone prevents oxidative stress, inflammation and hematological alterations, and modulates glutamate-nitric oxide-cGMP signaling in hyperammonemic rats. Biomed Pharmacother 102:392–402. https://doi.org/10.1016/j.biopha.2018.03.104
15. Hassanein EHM, Khader HF, Elmansy RA, Seleem HS, Elfiky M, Mohammedsaleh ZM, Ali FEM, Abd-Elhamid TH (2021) Umbelliferone alleviates hepatic ischemia/reperfusion-induced oxidative stress injury via targeting Keap-1/Nrf-2/ARE and TLR4/NF-kappaB-p65 signaling pathway. Environ Sci Pollut Res Int 28:67863–67879. https://doi.org/10.1007/s11356-021-15184-8
16. Jin T, Chen C (2022) Umbelliferone delays the progression of diabetic nephropathy by inhibiting ferroptosis through activation of the Nrf-2/HO-1 pathway. Food Chem Toxicol 163:112892. https://doi.org/10.1016/j.fct.2022.112892
17. Awoniran PO, Adeyemi DO (2018) Ethanol extract of Curcuma longa rhizome mitigates potassium bromate-induced liver changes in the Wistar rat: histological, histochemical and immunohistochemical assessments. Morphologie 102:276–288. https://doi.org/10.1016/j.morpho.2018.07.004
18. Naito H, Iba T, Takakura N (2020) Mechanisms of new blood-vessel formation and proliferative heterogeneity of endothelial cells. Int Immunol 32:295–305. https://doi.org/10.1093/intimm/dxaa008
19. Shi J, Barakat M, Chen D, Chen L (2018) Bicellular tight junctions and wound healing. Int J Mol Sci 19:3862. https://doi.org/10.3390/ijms19123862
20. Cialdai F, Risaliti C, Monici M (2022) Role of fibroblasts in wound healing and tissue remodeling on Earth and in space. Front Bioeng Biotechnol 10:958381. https://doi.org/10.3389/fbioe.2022.958381
21. McDougall S, Dallon J, Sherratt J, Maini P (2006) Fibroblast migration and collagen deposition during dermal wound healing: mathematical modelling and clinical implications. Philos Trans A Math Phys Eng Sci 364:1385–1405. https://doi.org/10.1098/rsta.2006.1773
22. Driskell RR, Watt FM (2015) Understanding fibroblast heterogeneity in the skin. Trends Cell Biol 25:92–99. https://doi.org/10.1016/j.tcb.2014.10.001
23. Thulabandu V, Chen D, Atit RP (2018) Dermal fibroblast in cutaneous development and healing. Wiley Interdiscip Rev Dev Biol 7:e307. https://doi.org/10.1002/wdev.307
24. Hata S, Okamura K, Hatta M, Ishikawa H, Yamazaki J (2014) Proteolytic and non-proteolytic activation of keratinocyte-derived latent TGF-beta1 induces fibroblast differentiation in a wound-healing model using rat skin. J Pharmacol Sci 124:230–243. https://doi.org/10.1254/jphs.13209fp
25. Huang J, Heng S, Zhang W, Liu Y, Xia T, Ji C, Zhang LJ (2022) Dermal extracellular matrix molecules in skin development, homeostasis, wound regeneration and diseases. Semin Cell Dev Biol 128:137–144. https://doi.org/10.1016/j.semcdb.2022.02.027
26. Bosman FT, Stamenkovic I (2003) Functional structure and composition of the extracellular matrix. J Pathol 200:423–428. https://doi.org/10.1002/path.1437
27. Abdallah F, Lecellier G, Raharivelomanana P, Pichon C (2019) R. nukuhivensis acts by reinforcing skin barrier function, boosting skin immunity and by inhibiting IL-22 induced keratinocyte hyperproliferation. Sci Rep 9:4132. https://doi.org/10.1038/s41598-019-39831-w
28. Chittasupho C, Manthaisong A, Okonogi S, Tadtong S, Samee W (2021) Effects of quercetin and curcumin combination on antibacterial, antioxidant, in vitro wound healing and migration of human dermal fibroblast cells. Int J Mol Sci 23:142. https://doi.org/10.3390/ijms23010142
29. Lamb MC, Tootle TL (2020) Fascin in cell migration: more than an actin bundling protein. Biology (Basel) 9:403. https://doi.org/10.3390/biology9110403
30. Van Audenhove I, Denert M, Boucherie C, Pieters L, Cornelissen M, Gettemans J (2016) Fascin rigidity and L-plastin flexibility cooperate in cancer cell invadopodia and filopodia. J Biol Chem 291:9148–9160. https://doi.org/10.1074/jbc.M115.706937
31. Lambrechts A, Kwiatkowski AV, Lanier LM, Bear JE, Vandekerckhove J, Ampe C, Gertler FB (2000) cAMP-dependent protein kinase phosphorylation of EVL, a Mena/VASP relative, regulates its interaction with actin and SH3 domains. J Biol Chem 275:36143–36151. https://doi.org/10.1074/jbc.M006274200
32. Baxter LL, Hou L, Loftus SK, Pavan WJ (2004) Spotlight on spotted mice: a review of white spotting mouse mutants and associated human pigmentation disorders. Pigment Cell Res 17:215–224. https://doi.org/10.1111/j.1600-0749.2004.00147.x
33. Tandara AA, Mustoe TA (2004) Oxygen in wound healing–more than a nutrient. World J Surg 28:294–300. https://doi.org/10.1007/s00268-003-7400-2
34. An Y, Liu WJ, Xue P, Ma Y, Zhang LQ, Zhu B, Qi M, Li LY, Zhang YJ, Wang QT et al (2018) Autophagy promotes MSC-mediated vascularization in cutaneous wound healing via regulation of VEGF secretion. Cell Death Dis 9:58. https://doi.org/10.1038/s41419-017-0082-8
35. Baroni A, Buommino E, De Gregorio V, Ruocco E, Ruocco V, Wolf R (2012) Structure and function of the epidermis related to barrier properties. Clin Dermatol 30:257–262. https://doi.org/10.1016/j.clindermatol.2011.08.007
36. Basler K, Bergmann S, Heisig M, Naegel A, Zorn-Kruppa M, Brandner JM (2016) The role of tight junctions in skin barrier function and dermal absorption. J Control Release 242:105–118. https://doi.org/10.1016/j.jconrel.2016.08.007
37. Furuse M, Hata M, Furuse K, Yoshida Y, Haratake A, Sugitani Y, Noda T, Kubo A, Tsukita S (2002) Claudin-based tight junctions are crucial for the mammalian epidermal barrier: a lesson from claudin-1-deficient mice. J Cell Biol 156:1099–1111. https://doi.org/10.1083/jcb.200110122
38. Kirschner N, Rosenthal R, Furuse M, Moll I, Fromm M, Brandner JM (2013) Contribution of tight junction proteins to ion, macromolecule, and water barrier in keratinocytes. J Invest Dermatol 133:1161–1169. https://doi.org/10.1038/jid.2012.507

39. Batista DI, Perez L, Orfali RL, Zaniboni MC, Samorano LP, Pereira NV, Sotto MN, Ishizaki AS, Oliveira LM, Sato MN et al (2015) Profile of skin barrier proteins (filaggrin, claudins 1 and 4) and Th1/Th2/Th17 cytokines in adults with atopic dermatitis. J Eur Acad Dermatol Venereol 29:1091–1095. https://doi.org/10.1111/jdv.12753
40. Yu HY, Yang IJ, Lincha VR, Park IS, Lee D-U, Shin HM (2015) The effects of the fruits of Foeniculum vulgare on skin barrier function and hyaluronic acid production in HaCaT keratinocytes. Journal of Life Science 25:880–888. https://doi.org/10.5352/jls.2015.25.8.880
41. Shin JW, Kwon SH, Choi JY, Na JI, Huh CH, Choi HR, Park KC (2019) Molecular mechanisms of dermal aging and antiaging approaches. Int J Mol Sci 20:2126. https://doi.org/10.3390/ijms20092126
42. Lee JO, Hwang SH, Shen T, Kim JH, You L, Hu W, Cho JY (2021) Enhancement of skin barrier and hydration-related molecules by protopanaxatriol in human keratinocytes. J Ginseng Res 45:354–360. https://doi.org/10.1016/j.jgr.2020.12.003
43. Farage MA, Miller KW, Maibach HI (eds) (2010) Textbook of aging skin, hyaluronan and the process of aging in skin, pp 225–238. https://doi.org/10.1007/978-3-540-89656-2
44. Prestwich GD (2011) Hyaluronic acid-based clinical biomaterials derived for cell and molecule delivery in regenerative medicine. J Control Release 155:193–199. https://doi.org/10.1016/j.jconrel.2011.04.007
45. Bollag WB, Aitkens L, White J, Hyndman KA (2020) Aquaporin-3 in the epidermis: more than skin deep. Am J Physiol Cell Physiol 318:C1144–C1153. https://doi.org/10.1152/ajpcell.00075.2020
46. Garcia N, Gondran C, Menon G, Mur L, Oberto G, Guerif Y, Dal Farra C, Domloge N (2011) Impact of AQP3 inducer treatment on cultured human keratinocytes, ex vivo human skin and volunteers. Int J Cosmet Sci 33:432–442. https://doi.org/10.1111/j.1468-2494.2011.00651.x

Publisher's Note Springer Nature remains neutral with regard to jurisdictional claims in published maps and institutional affiliations.